BRIEF REPORTS

Brief Reports are short papers which report on completed research or are addenda to papers previously published in the **Physical Review**. *A Brief Report may be no longer than four printed pages and must be accompanied by an abstract.*

Spin, moments, and mean square nuclear charge radius of ^{77}Sr

P. Lievens
ISOLDE Collaboration, CERN, CH-1211 Genève 23, Switzerland

L. Vermeeren
Instituut voor Kern- en Stralingsfysika, Katholieke Universiteit Leuven, B-3001 Leuven, Belgium

R. E. Silverans
Laboratorium voor Vaste Stof-Fysika en Magnetisme, Katholieke Universiteit Leuven, B-3001 Leuven, Belgium

E. Arnold, R. Neugart, and K. Wendt
Institut für Physik, Universität Mainz, D-6500 Mainz, Germany

F. Buchinger
Foster Radiation Laboratory, McGill University, Montreal, Canada H3A 2B2
(Received 23 March 1992)

The neutron deficient ^{77}Sr nucleus was studied by fast ion beam collinear laser spectroscopy with a detection scheme based on optical pumping, state selective neutralization, and atom counting. From the measured hyperfine splitting and isotope shift of the Sr II transition $5s\ ^2S_{1/2} \rightarrow 5p\ ^2P_{3/2}$ the nuclear spin $I=\frac{5}{2}$, the nuclear moments $\mu=-0.348(4)\mu_N$, $Q_s=1.40(11)$ b, and the change in mean square charge radius $\delta\langle r^2\rangle^{88,77}=0.248(12)$ fm^2 were deduced. These ground-state properties indicate a large prolate deformation of $\epsilon_2 \simeq 0.4$ and allow a comparison with calculations performed in the particle-plus-deformed-core model, assigning a $[422]\frac{5}{2}$ Nilsson configuration to the ground state of ^{77}Sr.

PACS number(s): 21.10.Ft, 21.10.Ky, 21.10.Hw, 27.50.+e

The region of the nuclear chart with about an equal proton and neutron number around the submagic shell gaps at $Z,N=38$ and 40 is known to exhibit a coexistence of strong prolate and strong oblate deformations in connection with a rapid transition from spherical to deformed shapes [1]. Several theoretical calculations indeed predict unusual shape fluctuations in this region [2–5]. For the neutron deficient strontium nuclei, studies of the nuclear level schemes revealed a very strong prolate ground-state deformation for the isotopes approaching $N=Z=38$ [6]. Only for the isotopes with $A \geq 78$, could values for the quadrupole deformation be extracted from lifetime measurements of low-lying excited levels.

Key information to identify the ground-state configuration of the odd isotopes is provided by the determination of the spin and the nuclear electromagnetic moments. Such detailed knowledge in combination with theoretical calculations will furthermore lead to reliable information about the nuclear ground-state deformation.

So far the series of strontium isotopes studied by laser spectroscopy reaches from ^{78}Sr to ^{100}Sr [7–11]. In this paper, an extension of these measurements towards the lightest known odd strontium isotope ^{77}Sr is reported. Fast-beam collinear laser spectroscopy with nonoptical detection was used to measure the hyperfine structure in the Sr II transition $5s\ ^2S_{1/2} \rightarrow 5p\ ^2P_{3/2}$. The method involves the detection of resonant laser-ion interaction in a three-step process [12]: optical depopulation pumping, in-flight state selective neutralization on an alkali vapor, and charge state separated atom counting. A refinement of this technique utilizing the strong dependence on the ion energy of the neutralization cross sections was used to discriminate the strontium ions from rubidium contaminations in the beam.

This Brief Report describes the experiment in more detail and presents the results and the extraction of the nuclear observables from the data. A discussion of the deformation of ^{77}Sr and an interpretation of the results by a comparison with calculations in the particle-plus-deformed-core model is given.

The experiment was performed on line at the mass separator ISOLDE 2 at CERN [13]. The neutron deficient strontium isotopes are produced in a spallation reaction induced by the irradiation of a Nb-powder target (50 g/cm^2) with 600-MeV protons. The reaction products diffuse out of the target into the surface ionization

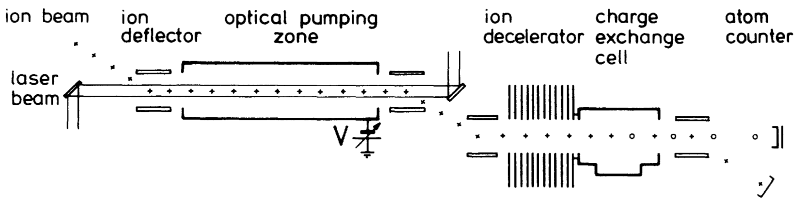

FIG. 1. Experimental setup for collinear laser spectroscopy on strontium ions with the nonoptical detection scheme based on optical pumping, state selective neutralization, and atom counting. The ions are slowed down before neutralization in order to reduce the rubidium contamination in the final atomic beam.

source. The produced ions are extracted by an electrostatic potential of 40 kV, leading to a ^{77}Sr [$T_{1/2}=9(1)$ s] beam intensity of $\simeq 10^5$ ions/s. The isobaric ^{77}Rb beam contamination is about 10^4 times higher ($\simeq 6\times 10^8$ ions/s).

Fast ion beam collinear laser spectroscopy is performed in the Sr II transition $5s\,^2S_{1/2}\rightarrow 5p\,^2P_{3/2}$ ($\lambda=407.9$ nm). The resonant interaction between laser photons and ions is detected via a three-step nonoptical detection scheme (see Fig. 1). Details of the method are presented in Ref. [12]. Optical depopulation pumping from the $5s$ ground state to the $5p$ state and subsequent decay populates the metastable $4d$ states. For these the neutralization cross section in collisions with sodium atoms is much larger than for ions in the ground state. Therefore, the ions are transmitted through a sodium vapor cell. The remaining ions and the atoms are electrostatically separated and counted by a secondary electron multiplier. The laser resonances then show up as peaks in the neutralized particle count rate.

Applied to pure beams of one isotope, this detection mechanism offers a considerable gain in overall sensitivity compared to fluorescent photon detection, as was illustrated by the measurements on ^{99}Sr and ^{100}Sr [9,11]. A strong contamination of the mass-separated beam with isobaric ions, however, produces a large background if the corresponding neutralization cross section is comparable to the one of the element under study. Therefore, the method had to be refined for the present experiment.

The impact energy dependence of the neutralization cross sections was exploited to reduce the Rb background count rate. This is illustrated in Fig. 2 where the experimental neutralization cross sections for $Sr^+(5s)$, $Sr^+(4d)$, and Rb^+ on Na are presented [14]. The Rb cross section becomes extremely small at low beam energy, while the Sr cross sections fall much more slowly with decreasing energy: the ratio $\sigma[Sr^+(5s)]/\sigma(Rb^+)$ increases from $\simeq 3$ at 30-keV energy to $\simeq 75$ at 5 keV. Therefore, the ion beam was decelerated to 5 keV prior to neutralization. Then, also, the cross-section ratio $\sigma[Sr^+(4d)]/\sigma[Sr^+(5s)]$ rises by a factor of about 2.5 resulting in a 100 times better total sensitivity [15].

The procedure for measuring the ^{77}Sr resonances is essentially the same as in the earlier collinear laser spectroscopy measurements on strontium isotopes [10]. The resonances are traced by Doppler tuning, i.e., by varying the voltage applied to a Faraday cage around the optical pumping region while the laser frequency is kept constant. For the isotope shift measurement, the resonances of the even isotopes ^{78,88}Sr are registered in the same measuring cycle.

The spectrum obtained for ^{77}Sr in a 40-s per channel measurement is given in Fig. 3. A least-squares fit assuming the nuclear spin $I=\frac{5}{2}$ leads to a χ^2 value of 120. With other spin assumptions, χ^2 is much higher (for $I=\frac{3}{2}$, $\chi^2=155$, and for $I=\frac{7}{2}$, $\chi^2=150$), thus giving strong support for the $I=\frac{5}{2}$ nuclear spin assignment. Furthermore, the observed line intensities are in perfect agreement with the predictions from rate equation calculations for $I=\frac{5}{2}$, which is not the case for other spin values. The final values for the hyperfine parameters are determined taking a fixed ratio $A(^2S_{1/2})/A(^2P_{3/2})=27.74$, known from the other Sr isotopes [10]. This yields $A(^2S_{1/2})=-573.8(30)$ MHz, $A(^2P_{3/2})=-20.7(2)$ MHz, and $B(^2P_{3/2})=370(15)$ MHz, and the isotope shift $IS^{88,77}=-960(18)$ MHz.

From the hyperfine parameters $A(^2S_{1/2})$ and $B(^2P_{3/2})$, the nuclear magnetic dipole moment and the nuclear spectroscopic electric quadrupole moment can be deduced using the values for ^{87}Sr as references [10]. This yields $\mu=-0.348(4)\mu_N$ and $Q_s=1.40(11)$ b. Apart from the error on the hyperfine parameter, the error on the magnetic moment includes an uncertainty of $0.002\mu_N$ introduced to account for the unknown hyperfine anomaly [16]. The main contribution to the error on the quadrupole moment stems from the uncertainty in the reference value for ^{87}Sr and is related to the determination of the atomic factor in B.

Following the procedure described in Refs. [9,10], the change in the mean square charge radius $\delta\langle r^2\rangle^{88,77}$

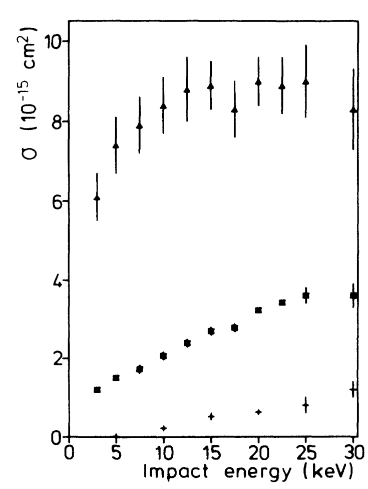

FIG. 2. Cross sections for neutralization of Rb ions (+) and ground state (■) and metastable state (▲) Sr ions on Na as a function of the impact energy as measured in [14].

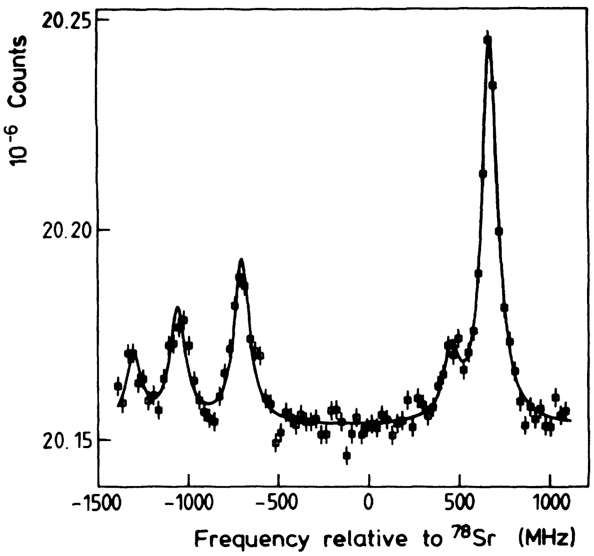

FIG. 3. Hyperfine split spectrum of the ionic transition $5s\,^2S_{1/2} \rightarrow 5p\,^2P_{3/2}$ of ^{77}Sr recorded by state selective atom counting in a 40-s per channel measurement.

$=0.248(12)[46]$ fm^2 was deduced from the isotope shift. The error between parentheses gives the experimental uncertainty (statistical error and error due to the voltage calibration), while the error between square brackets includes a systematic error due to the atomic parameters in the evaluation of the isotope shift.

Extensive information on the nuclear ground-state properties of the light strontium isotopes has been collected during the last decade [1]. The study of nuclear level schemes [6], the measurements of reduced transition probabilities ($BE2$ values) [17], as well as the laser spectroscopic studies in this region [7–10] show that the neutron deficient strontium isotopes gradually develop a very strong deformation far away from stability.

So far no quantitative measure of the ^{77}Sr deformation has been obtained. Our measurements of the nuclear spin and the moments allow the extraction of the quadrupole deformation parameter as well as an identification of the ground-state configuration by comparison with the calculated values from the LUND particle-plus-deformed-core model. A full description of the model and details of the calculation method can be found in [18]. In the modified harmonic-oscillator potential, the Nilsson parameters $\kappa_n=0.07$ and $\mu_n=0.40$ (ls and ll coupling) are used [19]. The pairing strength is taken as $GA=22-8(N-Z)/A$ MeV and $\sqrt{5N}$ orbitals above and below the Fermi level are included in the calculation. The moment of inertia is assumed to vary according to the formula

$$J_i=4B\epsilon_2^2 \sin(\gamma-\tfrac{2}{3}\pi i)\ ,$$

where B is calculated to reproduce the energy of the first excited 2^+ state of the even-even core, i.e., $E_{2^+}(^{76}\mathrm{Sr})=261$ keV [20]; $i=1,2,3$ denotes the intrinsic axes of the nucleus. In the calculation of the magnetic moment, the gyromagnetic ratios $g_R=Z/A$ and $g_s=0.6g_s^{\mathrm{free}}$ are used.

In a full quasiparticle-plus-deformed-core coupling calculation including the positive-parity orbitals originating from the $1g\frac{9}{2}$ shell and the downsloping $2d\frac{5}{2}$ and $1g\frac{7}{2}$ orbitals, good agreement between experimental and calculated level spacings for the ground-state band was found for a prolate quadrupole deformation $\epsilon_2=0.40$ (see Fig. 4). The spectroscopic quadrupole moment calculated at this deformation ($Q_s^{\mathrm{calc}}=1.375$ b) is in perfect agreement with the experimental value. The reproduction of the magnetic moment ($\mu^{\mathrm{calc}}=-0.611\mu_N$) is also satisfactory. The ground-state band is calculated to be of very pure Nilsson $[422]\frac{5}{2}$ character (only about 2% admixture of the $[431]\frac{3}{2}$ configuration). Therefore, a calculation with only this $[422]\frac{5}{2}$ orbital was carried out, yielding $Q_s^{\mathrm{calc}}(\mathrm{II})=1.470$ b and $\mu^{\mathrm{calc}}(\mathrm{II})=-0.318\mu_N$. However, the energy spacings in the band are then calculated too large (Fig. 4). This could be overcome by choosing a larger value for the moment of inertia, which would mean that ^{77}Sr is a more rigid rotor than the even-even neighbor ^{76}Sr, or by the introduction of an appropriate Coriolis attenuation. The strong dependence of the magnetic moment on small admixtures of the other orbitals in the wave function is due to the fact that the collective and single particle contributions cancel out to a large extent. Although a more detailed comparison with experiment of the particle-rotor calculations is not possible due to the lack of spectroscopic information at higher excitation energy, the results give an unambiguous identification of the ground state of ^{77}Sr with a $[422]\frac{5}{2}$ Nilsson configuration.

The very large deformation predicted by the particle-

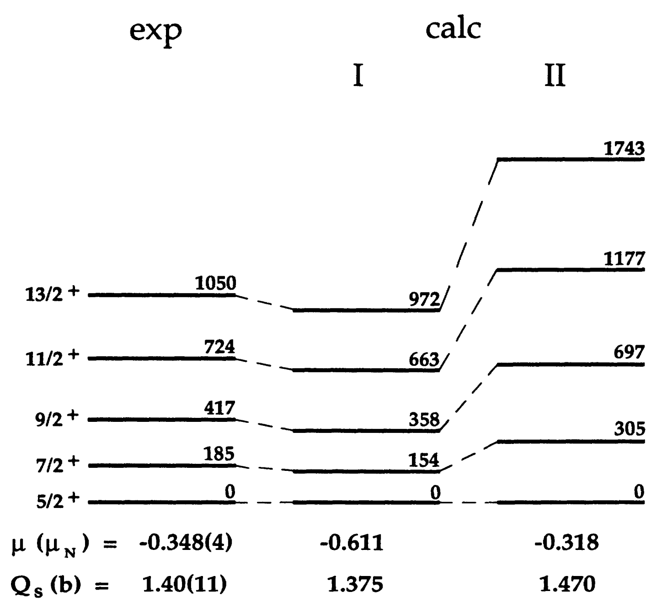

FIG. 4. Comparison of the experimental nuclear level scheme and nuclear moments with a calculation in the LUND particle-plus-deformed-core model assuming a quadrupole deformation $\epsilon_2=0.4$. The level energies are given in keV. (I) gives the full calculation taking into account all positive-parity orbitals close to the Fermi level, while (II) is restricted to the $[422]\frac{5}{2}$ Nilsson orbital.

rotor model is in perfect agreement with the measured quadrupole moment. This is also reflected in the validity of the strong-coupling limit which gives an intrinsic quadrupole moment $Q_0=3.92(31)$ b and $\epsilon_2=0.395(25)$ [21]. Moreover, the observed change in the mean square charge radius is reproduced by the droplet model [22] if this deformation is included in the procedure described in Ref. [9].

The authors wish to thank I. Ragnarsson for valuable discussions and for making available the LUND particle-plus-deformed-core model computer code. This work was supported by the Belgian Interuniversitair Instituut voor Kernwetenschappen (IIKW), the German Bundesministerium für Forschung und Technologie (BMFT) under Contract No. 06 MZ 188 I, and the Canadian Natural Sciences and Engineering Council (NSERC).

[1] *Proceedings of the International Workshop on Nuclear Structure in the Zr Region, Bad Honnef, 1988,* edited by J. Eberth, R. A. Meyer, and K. Sistemich (Springer-Verlag, Berlin, 1988).

[2] K. Heyde, J. Moreau, and M. Waroquier, Phys. Rev. C **29**, 1859 (1984).

[3] W. Nazarewicz, J. Dudek, R. Bengtsson, T. Bengtsson, and I. Ragnarsson, Nucl. Phys. **A435**, 397 (1985).

[4] P. Möller, W. D. Myers, W. J. Swiatecki, and J. Treiner, At. Data Nucl. Data Tables **39**, 225 (1988).

[5] P. Bonche, H. Flocard, P. H. Heenen, S. J. Krieger, and M. S. Weiss, Nucl. Phys. **A443**, 39 (1985).

[6] C. J. Lister, B. J. Varley, H. G. Price, and J. W. Olness, Phys. Rev. Lett. **49**, 308 (1982).

[7] M. Anselment, F. Bekk, S. Chongkum, S. Göring, A. Hanser, H. Hoeffgen, W. Kälber, G. Meisel, and H. Rebel, Z. Phys. A **326**, 493 (1987).

[8] D. A. Eastham, P. M. Walker, J. R. H. Smith, D. D. Warner, J. A. R. Griffith, D. E. Evans, S. A. Wells, M. J. Fawcett, and I. S. Grant, Phys. Rev. C **36**, 1583 (1987).

[9] R. E. Silverans, P. Lievens, L. Vermeeren, E. Arnold, W. Neu, R. Neugart, K. Wendt, F. Buchinger, E. B. Ramsey, and G. Ulm, Phys. Rev. Lett. **60**, 2607 (1988).

[10] F. Buchinger, E. B. Ramsey, E. Arnold, W. Neu, R. Neugart, K. Wendt, R. E. Silverans, P. Lievens, L. Vermeeren, D. Berdichevsky, R. Fleming, D. W. L. Sprung, and G. Ulm, Phys. Rev. C 41, 2883 (1990).

[11] P. Lievens, R. E. Silverans, L. Vermeeren, W. Borchers, W. Neu, R. Neugart, K. Wendt, F. Buchinger, and E. Arnold, Phys. Lett. B **256**, 141 (1991).

[12] R. E. Silverans, P. Lievens, and L. Vermeeren, Nucl. Instrum. Methods. B **26**, 591 (1987).

[13] H. L. Ravn and B. W. Allardyce, in *Nuclei Far from Stability,* edited by D. A. Bromley (Plenum, New York, 1988), Vol. 8, p. 363.

[14] L. Vermeeren, P. DeBisschop, P. Lievens, and R. E. Silverans, J. Phys. B **21**, 3417 (1988); L. Vermeeren, A. Bueckenhout, P. Lievens, and R. E. Silverans, *ibid.* **25**, 1009 (1992).

[15] P. Lievens, E. Arnold, W. Borchers, F. Buchinger, U. Georg, A. Klein, W. Neu, R. Neugart, M. Neuroth, C. Schulz, R. E. Silverans, and L. Vermeeren, Nucl. Instrum. Methods. B (in press).

[16] P. A. Moskowitz and M. Lombardi, Phys. Lett. **46B**, 334 (1973).

[17] S. Raman, C. W. Nestor, Jr., S. Kahane, and K. H. Bhatt, At. Data Nucl. Data Tables **42**, 1 (1989).

[18] S. E. Larsson, G. Leander, and I. Ragnarsson, Nucl. Phys. **A307**, 189 (1978).

[19] J. Rekstad and G. Løvhøiden, Nucl. Phys. **A267**, 40 (1976).

[20] C. J. Lister, B. J. Varley, W. Gelletly, A. A. Chishti, A. N. James, T. Morrison, H. G. Price, J. Simpson, and O. Skeppstedt, *Nuclei Far from Stability,* Proceedings of the 5th International Conference on Nuclei far from Stability, AIP Conf. No. 164, edited by I. S. Towner (AIP, New York, 1988), p. 354.

[21] K. E. G. Löbner, M. Vetter, and V. Hönig, Nucl. Data Tables **A7**, 495 (1970).

[22] W. D. Myers and K. H. Schmidt, Nucl. Phys. **A410**, 61 (1983).